Late Holocene sedimentary response to solar and cosmic ray activity influenced climate variability in the NE Pacific

R. Timothy Patterson[a,*], Andreas Prokoph[b], Alice Chang[a]

[a]Department of Earth Sciences and Ottawa-Carleton Geoscience Centre, Carleton University, Ottawa, Ontario, Canada K1S 5B6
[b]SPEEDSTAT, 36 Corley Private, Ottawa, Ontario, Canada K1V 8T7

Abstract

Marine-laminated sediments along the NE Pacific coast (Effingham inlet, Vancouver Island) provide an archive of climate variability at annual to millennial scales. A 7.75-m portion of piston core TUL99B-03 was deposited during a ~3045-year interval [~1440–4485 years before present (yBP)] under primarily anoxic conditions. Darker clay laminae were deposited under higher precipitation conditions in winter, and diatom-dominated laminae were laid down when marine productivity was higher in the spring through autumn.

Wavelet transform and other time-series analysis methods were applied to sediment color (i.e. gray-scale values) line-scans obtained from X-ray images and compared with global records of cosmogenic nuclides ^{14}C and ^{10}Be, as well as the Ice Drift Index (hematite-stained grains) record to detect cycles, trends, and nonstationarities in the climate and sedimentary pattern. Our results show that the marine sedimentary record in the NE Pacific responded to abrupt changes and long-term variability in climate that can be linked to external forcing (e.g., solar and cosmic irradiance). Specifically, a strong cooling in the NE Pacific at ~3550±160 yBP can be correlated to a weakening of high-frequency (50–150 years) pulses in sun activity at the Gleissberg cycle band, similar to what occurred at the onset of the 'Little Ice Age' at ~1630 AD.

Three intervals of unusually low sun activity at ~2350, 2750, and ~3350 yBP are characterized by thick, clay-rich annual sedimentation that we interpret as representative of unusually wet conditions. These intervals of higher precipitation conditions may have been related to a regional intensification of the Aleutian Low (AL) caused by an eastward migration of the Center of Action (COA) of the AL, which occurs during intervals of solar minima. Dryer conditions in the region occur when the COA of AL migrates westward and the COA of the North Pacific High (NPH) migrates northward during intervals of solar maxima. A cyclicity of 50–85, 33–36, and 22–29 years in the sediment color record, lamination thickness, and ^{14}C cosmogenic nuclide, characterized the relatively warm interval from 3550 to 4485 yBP. This record is similar to that of present-day low- and high-frequency variants of the Pacific Decadal Oscillation and Aleutian Low.
© 2004 Elsevier B.V. All rights reserved.

Keywords: NE Pacific; Laminated sediments; Wavelet transform; Cyclicity; Solar irradiance; Climate change

* Corresponding author. Tel.: +613 520 2600x4425; fax: +613 520 2569.
   E-mail address: tpatters@ccs.carleton.ca (R.T. Patterson).

1. Introduction

Effingham Inlet, Vancouver Island, British Columbia, has proven to be an ideal area to carry out cyclostratigraphic research as cores collected from the inlet are characterized by annually deposited, finely laminated sediments that were deposited under generally anoxic (oxygen-free) and dysoxic (low oxygen) bottom water conditions (Chang et al., 2003). Benthic organisms are absent under these conditions so there is no bioturbation of the sediments. The preserved laminations represent the seasonal accumulation of

different particle types from the water column (Chang et al., 2003). In addition, there is a direct response of the resident waters within Effingham Inlet to conditions in the open ocean as it is contiguous with the eastern North Pacific (Thomson, 1981).

We present evidence of a link between the pattern of marine sedimentation within Effingham Inlet, west coast of Vancouver Island, British Columbia (Fig. 1), and regional to global climate changes that appear to be driven by fluctuations in solar and cosmic ray activity. The laminated sediments can archive ultra-high resolution information, providing valuable data
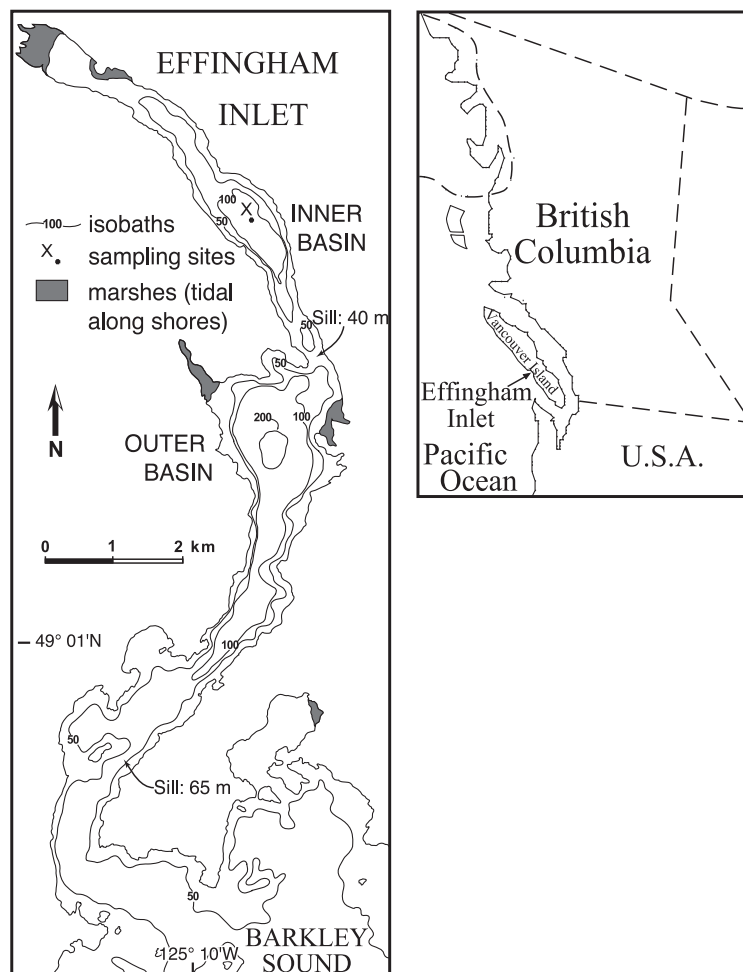

Fig. 1. (A) Location map of southern British Columbia (modified after Favorite et al., 1976) showing geographic features discussed in this paper. (B) Details of Effingham Inlet showing location of piston core TUL99B-03 collected in the inner basin.

on seasonal scale processes as well as intra- and inter-annual variability. In Effingham Inlet, laminated Holocene sediments were deposited under conditions of moderately high marine primary productivity in the surface waters as indicated by abundant diatom remains in the sediments (Chang et al., 2003). We used our data set of digitized laminae thickness, and gray-scale variation, which relates directly to annual precipitation (winter laminae) and annual productivity (summer diatom laminae), to compile an extensive time-series that forms the basis for application of our wavelet transform and spectral analysis techniques.

2. Background

2.1. Ocean and atmospheric influences on climate in the NE Pacific

The major atmospheric climate forcing factors in the NE Pacific region off the west coast of North America are interdependent changes in the Aleutian Low (AL), the North Pacific High (NPH), the Jet Stream, and the equatorial El Niño/La Niña cycle. Less well-understood, regionally modified, decadal and centennial scale cycles, which appear to arise from global-scale teleconnections are superimposed on these weather phenomena (Mann et al., 1995; Ware and Thomson, 2000).

One of these longer cycles, the Pacific Decadal Oscillation (PDO) is a decadal-scale oceanic index of Pacific Ocean sea surface temperatures that waxes and wanes in two general periodicities, one from 15 to 25 years and the second at 50–70 years (Minobe, 1997, 1999). A positive PDO coincides with warm water off the west coast of North America and a cool water pool in the central North Pacific. These conditions, in turn, coincide with reduced coastal upwelling, stronger poleward winds off the west coast and a strengthened Aleutian Low. The resultant changes in coastal nutrient supply and water temperature directly impact phytoplankton productivity, and subsequently higher trophic levels (Francis et al., 1998).

Under AL-dominant conditions downwelling is prevalent along the west coast of Vancouver Island, while NPH dominance results in the upwelling of cold, nutrient-rich continental slope water, stimulating

high primary productivity within many phytoplankton groups, particularly diatoms (Fig. 2).

2.2. Solar and cosmic ray influences on climate

A growing body of sedimentary and biological studies indicates that extraterrestrial factors are at least partially responsible for climate variability on scales ranging from days to millennia (e.g., Haigh, 1994; Mann et al., 1995; Soon et al., 1996; Pellat and Mathewes, 1997; Svensmark, 1998; Bond et al., 2001).
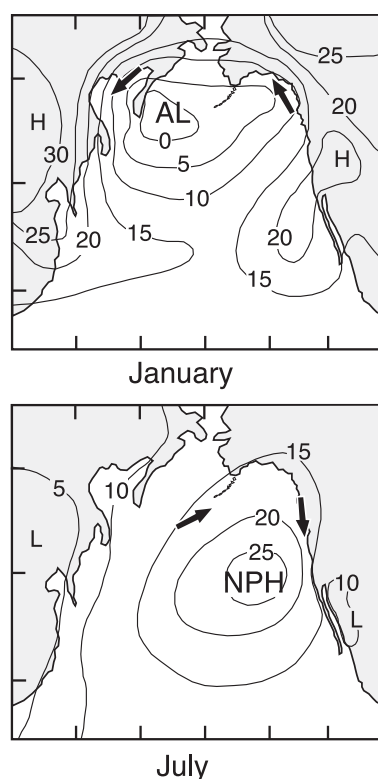

Fig. 2. (A) Main features of upwelling-favorable wind conditions off the British Columbia coast during the summer: Northerly North Pacific High (NPH) winds generate the southward Shelf-Break Current at the surface, and a consequent offshore Ekman transport inducing upwelling, thus bringing high-salinity deep water closer to the surface. (B) Main features of wind-induced downwelling off the west coast of Vancouver Island during winter: Southerly Aleutian Low (AL) winds generate a northward drift (NE Pacific Coastal Current or Davidson Current) and a consequent onshore Ekman transport. This causes an accumulation of low density less saline water on the surface, thus restricting the upwelling of deep water (modified after Thomson, 1981).

From observational records, the influence of solar irradiance and cosmic ray variability on global climate is well constrained at the frequency of the ∼ 9–12-year Schwabe sun spot cycle (Friis-Christiansen and Lassen, 1991). In addition, the ~20–22-year Hale Cycle, and the ~72–90-year Gleissberg sunspot cycle (Gleissberg, 1958; Garcia and Mouradian, 1998) are part of a well-documented amplitude modulation of the Schwabe cycle (Dean, 2000). Variability in the level of solar irradiance striking the earth through the Schwabe sunspot cycle has now been demonstrated to influence global sea-surface temperature (SST) fluctuation, including those of the Pacific ocean, by up to 0.4 °C (Jones et al., 2001). This is because an increase in solar activity results not only in enhanced thermal energy flux but more intense solar wind that attenuates the cosmic ray flux reaching Earth (Carslaw et al., 2002). Coeval fluctuation in the production rates of the cosmogenic nuclides ^{14}C and ^{10}Be, and annual to millennial time-scale changes in globally distributed proxies of drift ice suggest that celestial forcing plays a dominant role at centennial (~200–500 years) and at the millennial-scale (1000–1500 years) Bond cycle frequencies (Bond et al., 2001).

Previous research in coastal British Columbia has found evidence of significant climate fluctuations in cycles of 9–15 years (~11-years) Schabe Sunspot Cycle, ~20–30-year Bidecadal Oscillation (BDO), and 60–80-year Multidecadal or Very Low Frequency (VLF) Oscillation (Ware, 1995; Ware and Thomson, 2000; Gedalof and Smith, 2001). A late Quaternary–Holocene marine record from Saanich Inlet, SE coast of Vancouver Island (Nederbragt and Thurow, 2001) showed evidence of abrupt climate shifts from wet to dry conditions at ~3250 yBP, and back to wet at ~2100 yBP, but no evidence for cyclic solar forcing.

3. Data and methods

We extracted and analyzed two signals, sediment gray-scale values, and lamination thickness data from X-ray sediment images of core TUL99B-03. These signals were transformed from the core-depth scale into a time-scale by tying counts of the annual laminations in with six ^{14}C ages that were obtained through a ~9-m core interval. The uppermost and lowermost parts of the 12-m core were not assessed as sediments from the top (0–145 cm) and bottom (920–1135 cm) of the core were more homogenous, being characterized by a high percentage of earthquake-disturbed sediments, or non- to poorly laminated sediments due to bioturbation. In the aftermath of bottom water oxygenation event (Dallimore, 2001).

Laminae couplet counting started at a depth from which a reliable ^{14}C age was available (553 cm=2980 yBP) with lamination couplet thickness varying between 0.08 and 0.6 cm. Couplets were counted through the laminated intervals successively up and down-core from this tie point. The, counted ages were then compared with other radiometric ^{14}C ages through the core. The sediment ages based on lamination counts are within the limits of the average standard error associated with the radiocarbon dates of ± 158 years for 95% (2σ) confidence (Dallimore, 2001). Finally, the equal-distance X-ray grey values from line scan and the thickness of lamina couplet data were transformed into equidistant annual time intervals Δt=10 years and Δt=2 years by using a standard linear interpolation technique, as the focus of the research was to assess the influence of solar radiation and long-term climate fluctuations on time-scales >20 years.

The derivation of a detailed time scale permitted us to separate sediment color (=sediment chemistry and texture) from the sedimentation rate (=lamina couplet thickness) signals, and to assess productivity signals based on the ratio of mineral input (dark laminations) and diatom production (light-colored laminations) (Fig. 3). The methodology used in this study primarily involves image analysis and statistical analysis techniques of the sedimentary and other data (Fig. 4). We used time-series analysis techniques (wavelet analysis, spectral analysis and cross-spectral analysis) to determine persistence, wavelengths (periodicities), and confidence intervals of sedimentary and ^{14}C productivity cycles at age frequency bands between 15 and 3050 years.

3.1. Stratigraphy

Independent confirmation that the observed laminations were deposited annually has been provided by ^{14}C and detailed diatom analysis of core TUL99B-03 (Chang et al., 2003).
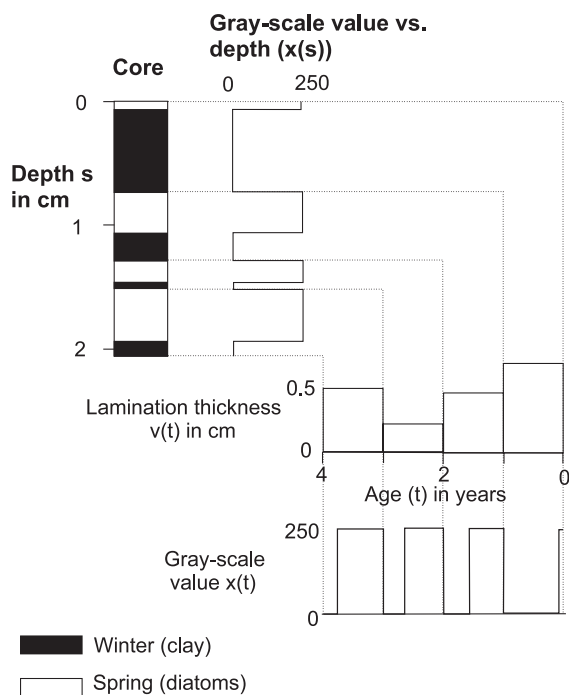
Fig. 3. Cartoon summarizing the loss of possible independence of variability in lamination thickness (total annual sediment accumulation) and of the variability in sediment color (gray-scale value) as ratio for clay mineral/ diatom percentage in a sediment column. Note that lamination thickness and gray-scale values may vary at different frequencies that are nonlinearly altered in the sediment column.

Dates presented are reported in radiocarbon years before present (yBP) and based on lamination counting (Table 1; Fig. 5). Radiocarbon dating results were calculated by IsoTrace Radiocarbon Laboratory using their C^{14}Cal program (Stuiver and Reimer, 1993; Stuiver et al., 1998a,b) along with the INTCAL98 dendrochronological database for terrestrial material, and the MARINE98 database for marine material (Stuiver et al., 1998a,b). The calibrated marine shell dates were not used in the determination of the sediment accumulation rate though as the marine reservoir effect has not been definitively established for restricted fjords such as Effingham Inlet on the coast of British Columbia (Beukens, personal communication, 2002).

Three accurate ^{14}C ages from wood fragments and twigs from core TUL99B-03 (Table 1) (Dallimore, 2001) indicate that the sedimentation rate was on average ~2.25 cm/year in the examined core interval (Fig. 7). Including the two ^{14}C ages from bivalve shells,
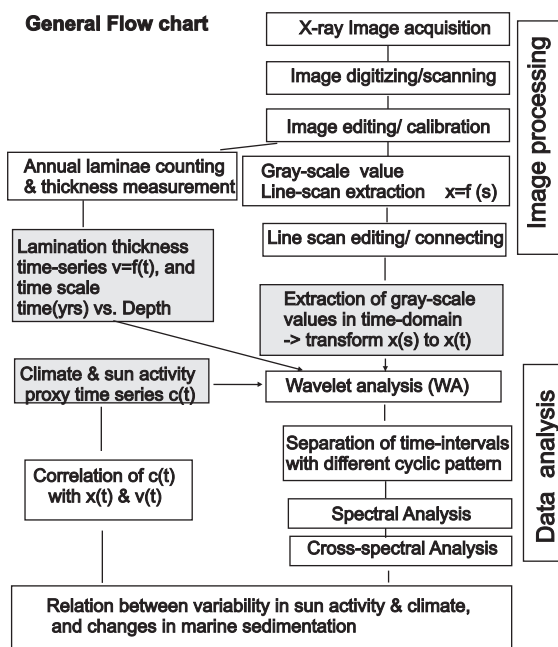

Fig. 4. Flow chart of image and data analysis methods used. Gray shaded fields mark data sets used or created during study.

the sedimentation rate would slightly increase to ~2.5 mm/ year (Fig. 6). Most of the ages from lamina couplet counts, except the youngest age at 97 cm, fit well into the depth-age model (Fig. 6). Detailed sedimentological and ^{14}C analysis of seven piston cores collected

Table 1
Radiocarbon versus varve count dating, TUL99B03

Depth (cm)	Radiocarbon (year BP)	Dated material	Counted age (year BP)	sr (cm/year) radiocarbon	sr (cm/year) varve counts
97	195 ± 150[a]	wood	N/A	0.06	N/A
169	1495 ± 160[b]	sea shells	1483	0.32	0.207
286	1858 ± 62	twig	2049	0.24	0.268
553	2980 ± 150	twig	3045	0.24	0.251
822	4085 ± 245[b]	sea shells	4118	0.17	0.237
937	4745 ± 175	wood	4603		
			sr mean (920–145 cm)	0.240	0.254

sr—sedimentation rate between radiocarbon-dated intervals (set to row of older age).
[a] Age of low probability (analytical uncertainties high).
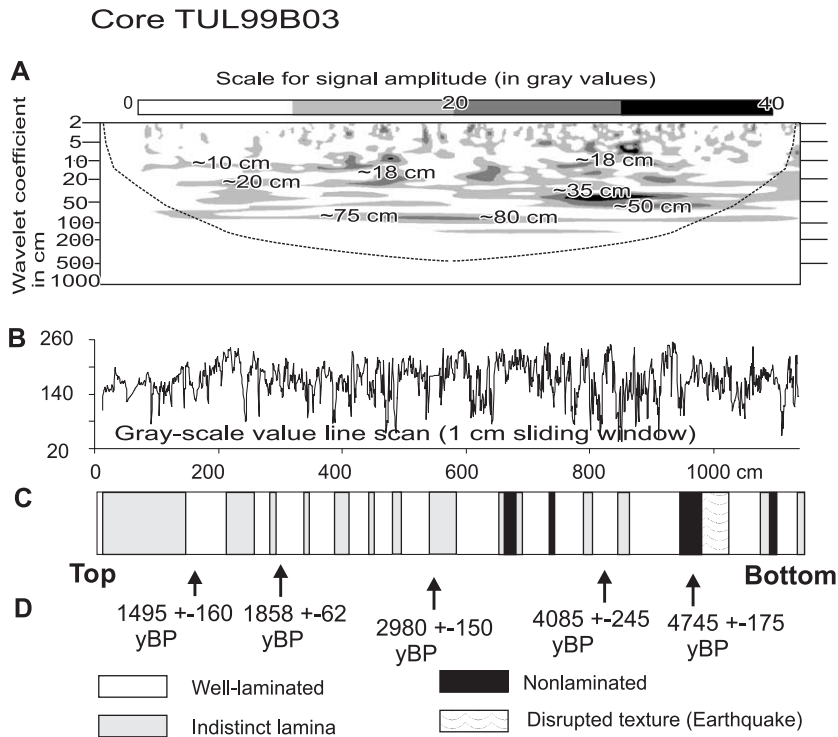[b] Using water residence time CAL (120 ± 45 years).

Fig. 5. Core TUL99B03: (A) Wavelet analysis (using Morlet wavelet with window size=10) of gray-scale value (='sediment color') line scan time series. Wavelet coefficients are scaled to maximum amplitude for highlighting of local variability (which is low on top and high on bottom). Dashed line shows 'Cone of influence' (Torrence and Compo, 1998) of edge effects. Gray-scale represents magnitude of wavelet coefficients in four levels. Numbers in scalogram indicate wavelengths that are repetitive for at least five times with bandwidth variability of less than ±5%. (B) Smoothed gray-scale value line scan of X-ray image of complete core. (C) Generalized lithologic variability of mixed biotic and clastic sediments (after Dallimore, 2001; Chang et al., 2003). (D) INTCAL98-Calibrated radiocarbon ages (after Dallimore, 2001). Note that the original X-ray line-scan data set of 130,790 data points has been used for annual gray-scale value extraction.

from throughout Effingham Inlet as part of a broader study revealed nearly identical stratigraphic successions in all cores (Dallimore, 2001), so that the patterns recognized in piston core TUL99B-03 are consistent with actual depositional conditions. However, correlations with the other piston cores (Dallimore, 2001) suggest that the last ~500 years of the ~5200-year total sediment record was not recovered due to overpenetration of the piston corer.

3.2. Data sets

There was a 97% recovery rate in the 775-cm (145–920 cm) interval of Core TUL99B-03 examined. This segment was comprised of 85% well-laminated sediments with the balance being non-laminated. A set of 39 slabs, ~20 cm long, 3 cm wide, and 1 cm thick, were taken for X-ray analysis using a sediment slab extraction device to ensure consistent sediment thickness. The scanned X-ray positive images were digitized at a resolution of 116 pixels/cm, providing 90,510 pixels along the depth axis for the entire core. Of this data, 92.6% (83,810 pixels) proved useful for time-series analysis. The remaining 7.4% of the core data could not be used because of missing core, poor image quality, or other factors.

Thin section microscope images (1000 pixels/cm) and backscattered electron microscopy (BSEM) images (12,500 pixels/cm) of selected intervals were examined to identify annual and multi-annual variation of litho- and biofacies, as well as to quantitatively assess the relationship between X-ray image gray-scale value variation and biotic and mineral composition.
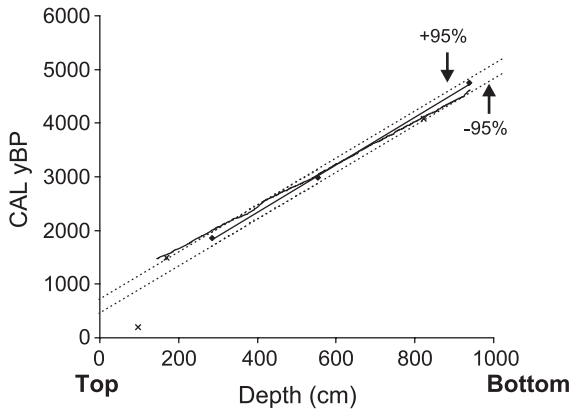
Fig. 6. Age-depth model (linear regression as bold straight line) of core TUL99B-03 based on three ^{14}C ages from twigs/wood at 286, 553, and 937 cm as diamonds. Other ages (see Table 1) are passively plotted (crosses). 95% confidence interval of regression line is based on error in ^{14}C ages (dotted lines). Fine solid line: Refinement of age-depth model based on counts and thickness of varves determined from X-ray images (for detail, see text). Note that the slope of the regression line is slightly steeper than the varve-thickness-based refinement.

Smoothed and detrended time-series data from Effingham Inlet was correlated with additional proxies such as ^{14}C production rate, ^{10}Be production rate, hematite-stained-grain (HSG) percentage in marine sediment (from Bond et al., 2001) to provide a more accurate paleoenvironmental interpretation.

3.3. Image processing

All digital images were generated in TIFF-Format and then edited with the image processing software IMAGEJ. Variations in the image background gray-scale values were transformed to equal standard values by using trend lines (Nederbragt and Thurow, 2001). Gray-scale color value measurement of laminations were derived from BSEM imagery and were generated by averaging swaths analyzed perpendicular to sedimentation at three resolutions; 3 pixel wide X-ray swaths, 40 pixel wide thin section swaths, or 400 pixel wide swaths. Further editing of all line scans involved correcting depth values from pixel numbers, and replacing extreme gray-scale values resulting from small cracks or concretions in the sediments by using linear interpolated values of the adjacent gray-scale values (after Schaaf and Thurow, 1994).

4. Results

4.1. Temporal sedimentary patterns in TUL99B-03 from digital images

Major seasonal changes from mineral to diatom-dominated deposition were well pronounced in the X-ray images obtained from core TUL99B-03. Laminations were easily detectable and could be counted manually from the X-ray images (Fig. 7A). The annual variation from dark winter layers to bright summer layers was the most distinct gray-scale value change (ranging from 0 (black) up to 255 (white)) and provided most (>75%) of the recognizable gray-scale value variance. However, due to the lower resolution at which X-ray line scans were captured, intraseasonal debris layers were not recognizable in these images (Fig. 7D). Examination of higher resolution BSEM images were required to reveal details of the pronounced variability in intraseasonal deposition within the inlet (Fig. 7C). Mineral-rich layers (clay and quartz) deposited during the winter months appear bright (gray value >100), while diatoms, deposited during blooms between spring and the autumn, appear dark in the BSEM images (Fig. 7C).

In general, sedimentary conditions are characterized by seasonal changing flux of clastic sediments from river runoff in winter and diatom sedimentation during spring–summer under anoxic bottom water conditions. Occasionally, storms, and heavy rains changed circulation patterns resulting in bottom water oxygenation, bioturbation, and graded sedimentation due to generation of bottom currents.

Because of the good correlation with the BSEM and thin sections obtained from Effingham Inlet cores, the gray-value variations from the X-ray images were easier to interpret than those obtained during Ocean Drilling Project Leg 169S in nearby Saanich Inlet, ~50 km to the southeast (Nederbragt and Thurow, 2001). Additional sublaminations, up to five in Saanich Inlet, hampered recognition of distinct annual laminations and made climate cycle recognition difficult (Blais-Stevens et al., 2001).

In addition to annual laminations showing bright and dark layer variation, longer sections of core TUL99B-03 displayed long and short-term time series patterns in the examined 145–920-cm core interval
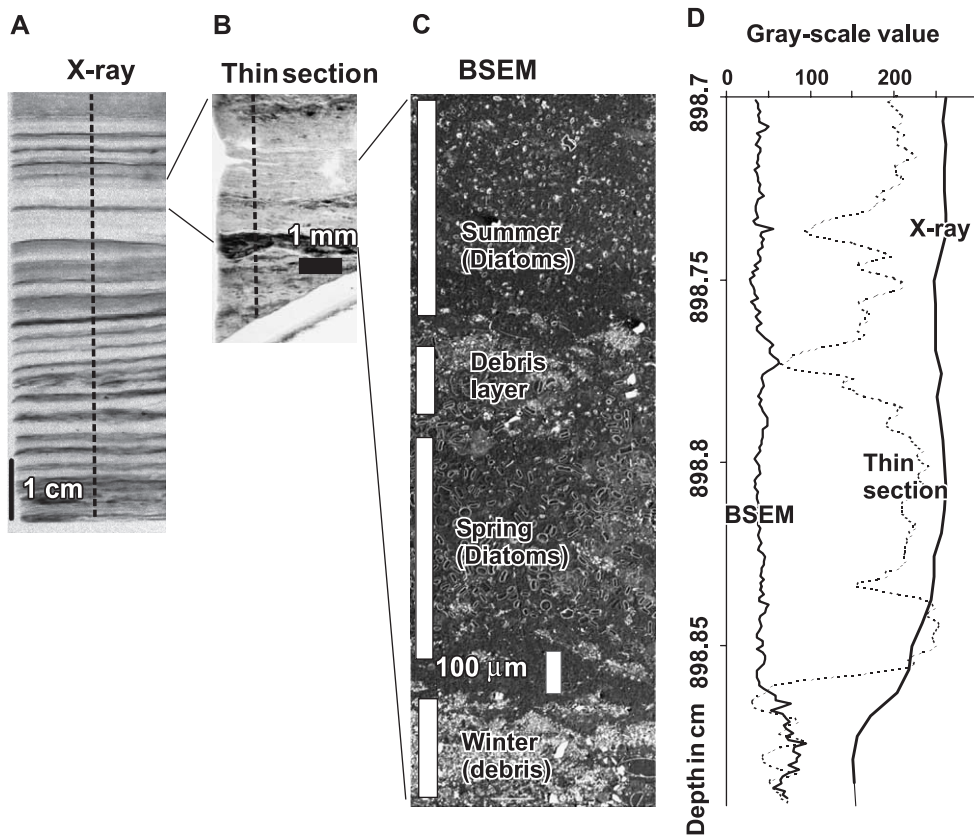
Fig. 7. Graphic correlation of digital image output from 898.7 to 898.89 cm depth of core TUL99B-03: (A) X-ray image (1 cm=116 pixel, line scan width: 3 pixel). (B) Thin section image (resolution: 1 cm=1000 pixel, line-scan wide: 40 pixel). (C) BSEM image (resolution: 1 cm=12,500 pixel, line scan wide: 400 pixel), diatoms are represented by bright colors in X-ray and thin section (gray-scale value >200) and debris layers by dark colors (gray-scale values <100). (D) Line-scan outputs of sediment color (gray value). The annual winter layer (clay minerals and quartz) occurs from ~898.86 to 898.89 cm, and sub-annual debris layers appear from ~898.77 to 898.778 cm, and weaker, from 898.74 to 898.743. Note that the correlation of the line scans is almost perfectly positive or negative, but X-ray resolution does not recognise thin sub-annual debris layers.

(Fig. 5). Bright sediments were particularly common at ~700, ~550 and ~220 cm depth. These bright sediments dominated the more poorly laminated sediments, which have been interpreted to correspond with episodes of higher sea floor oxygenation and increased bioturbation during deposition (Dallimore, 2001). Wavelet analysis of the gray-value from the X-ray images of the entire core indicates low sediment color variability through the top ~145 cm where non-laminated intervals prevail (Fig. 5). Wavelet analysis also indicates 60, 35, 28, 20, 18 and 11 cm cyclicity in different parts of the core with amplitudes of up to 40 gray-scale units that are, according to a mean (constant) sedimentation rate of 0.25 cm/year, roughly

equal to 310, 145, 110, 84, 75, and 45 years, respectively.

Detailed analysis of thin section images from these sections revealed that these, non-laminated intervals still contain the remains of primary lamination, which have a similar thickness range (0.2–0.4 cm) as adjacent well-laminated varves (Fig. 8). The mean gray value (~130), and thus mineralogical and biotic composition of the layers, was also similar to that of adjacent laminated layers. Although the gray-scale value variability inside the massive intervals was reduced, line scan analysis still permitted discrimination of laminations. Thus, for determination of the depth–time transform, the lamination thickness and
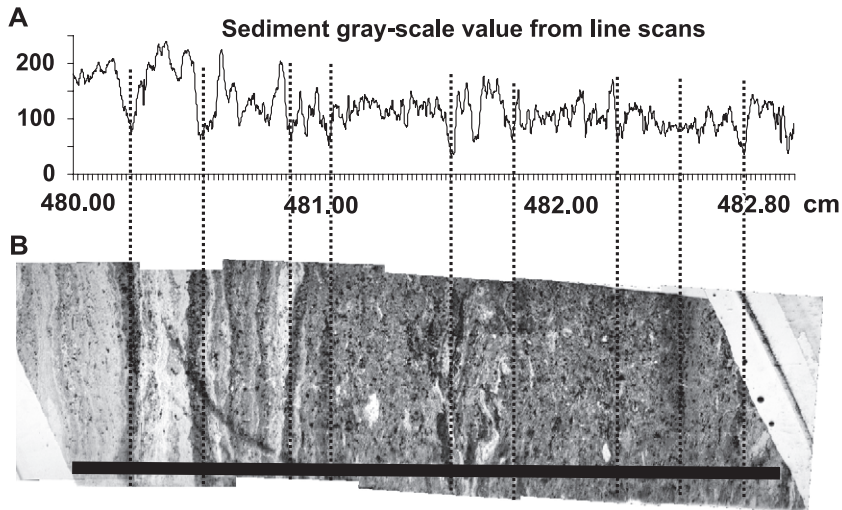
Fig. 8. Massive interval from a 2.85-cm section of core TUL99B-03: (A) Digital gray-scale value line scan (1 cm=1000 pixel). (B) Thin section image with 'massive interval'. The black line marks width (40 pixel) and location of the digitized scan. Note that a residual annual lamina structure is weakly preserved. Note also that three sub-annual layers weakly occur inside annual laminae from 480.5 to 480.9 cm depth.

gray-scale values for massive layers could be interpolated from the laminated sediments that bounded these units.

4.2. NE Pacific sedimentation versus global climate and solar irradiance variability

The time-series analysis carried out here covers the time-interval between ~1440 and 4485±160 yBP (145 to 920 cm depth) in the core (Fig. 9). [14]C production rate (detrended), lamination thickness and sediment color correlated well through the section; varying around their mean through the long-term (>1000 years) (Fig. 9E–G). There were deviations from the general long-term trend though. For example there were significant increases in ^{14}C production rate (i.e. lower solar irradiance levels) at ~3350, ~2750 and ~2350 yBP.

Both the sedimentary record and the ^{14}C production rate between ~4485 and 3550 yBP show a strong high-frequency cyclicity in the ~135- and 60–65-year bands with less intense cycles in the sedimentary record at ~60–90, 30–35 and ~15 years (Fig. 10). This cyclic pattern broke down in less than 100 years at ~3550 yBP being replaced by dominant cycles in ~200–500-year range (Fig. 10). The ~200-year wavelength cycles begin to weaken after ~2050 yBP, eventually giving way to ~60-year cycles in all records, as well 35-year cycles in the sedimentary record (Fig. 10).

Spectral and cross-spectral analysis (at Δt=10 years) throughout the ~3045-year record shows significant cyclicity at several frequency bands for ^{14}C production rate and sedimentation (Fig. 11). Our interpretation focuses on the >95% confident cross-correlations with ^{14}C production rate for period between 20 and 600 years. Longer periods are statistically not robust in a ~3050-year record and <20-year periods are below the Nyquist frequency.

A ~500 (508±45)-year bandwidth periodicity correlation between ^{14}C production rate and lamination thickness is significantly correlated (r^2=0.78). This cyclicity is most pronounced from ~2200 to 3500 yBP and correlates with cycles in the late Holocene Neoglacial advance phase (Bond et al., 2001; Figs. 9 and 10). It is possible that the ~500-year cyclicity may be driven by cosmic/solar activity but as these cycles are rather non-stationary, they are difficult to predict.

Significant cyclicity in the ~250–300-year period occurs in the sediment color record and a 45–48-year period occurs in lamination thickness. However, neither cycle correlates with the ^{14}C production rate, and are therefore the result of environmental factors that are not related to cosmic and/or solar forcing.

A wavelength of 190 ±6 years in ^{14}C production rate and lamination thickness (Fig. 11) is significantly correlated (r^2=0.78) at 2.67 radians (i.e. high [14]C
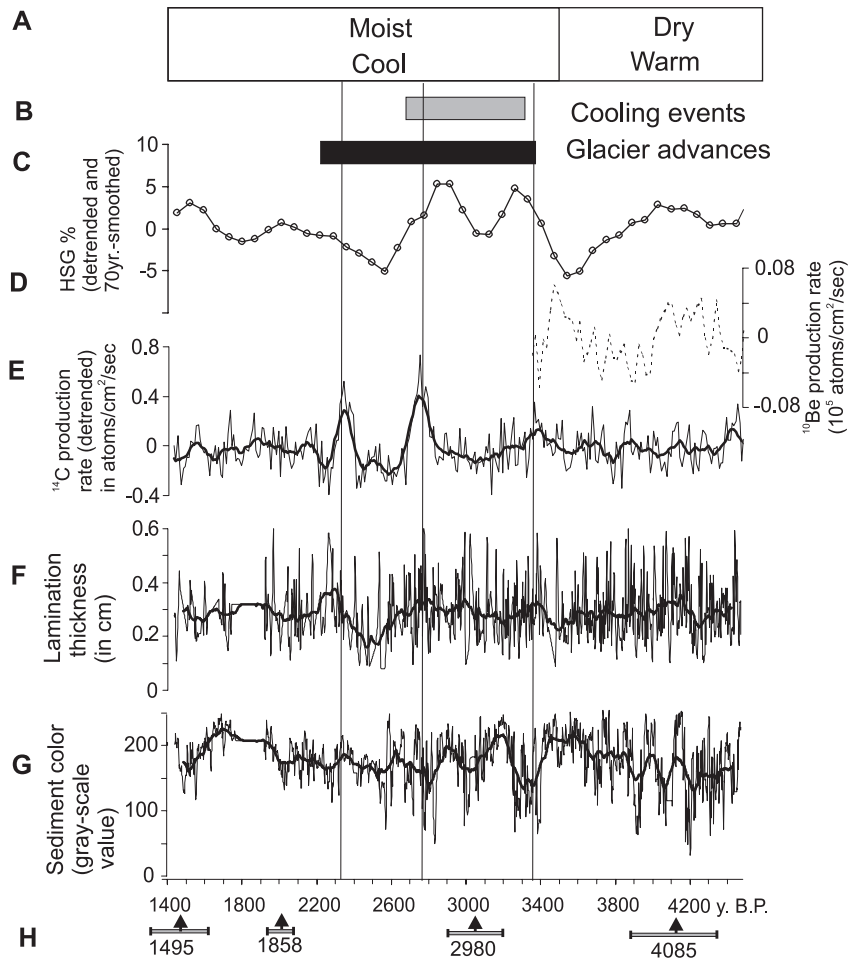
Fig. 9. Comparison between (A) climate stages and (B) Glacier advances ('Tiedemann', 'Peyto', 'Robson') on Canadian Pacific Coastline (after Pellat and Mathewes, 1997). (C) Global glacier advances. (D) Hematite stained grains (HSG) in percent sediment as an ice drift index in marine sediments. (E) [10]Be (dashed line) and ^{14}C detrended production rate with 100 year moving average (bold line) (after Bond et al., 2001). (F) Two-year mean lamination thickness rate with 100 year moving average (bold line) (this study). (G) Two-year mean sediment color (gray-scale value) with 100 year moving average (bold line) of TUL99B-03 (this study). (H) Time scale used (for details, see text) and INTCAL98 calibrated ^{14}C ages with 2σ-confidence intervals. Three vertical lines trace the major cooling events (see Bond et al., 2001) into all time-series.

production rate and low solar irradiance). Like the ~500-year cycle, the ~190-year cycle only occurs between ~2050 and 3550 yBP in the records (Fig. 10).

Cyclicity in ^{14}C production rate is significantly cross-correlated with lamination cyclicity thickness at 27.5 ± 0.2 and $\sim 127 \pm 3.5$; and with cyclicity in sediment color at 138 ± 3.8 (Fig. 11). The time-scale calibration between sedimentation and ^{14}C production rate records is not good enough to draw any conclusion from the phase shifts though, or to determine any possible direct environmental effect of solar radiation changes.

There is an 80–85-year cyclicity in all records (Fig. 11). The results suggest that solar irradiance and/or cosmic ray flux changes have had more impact on annual sediment accumulation than on the sediment color.

4.3. Detailed time series analysis

Based on the results of wavelet analysis, three time periods were separated for detailed spectral analysis; 1440–2050 $\pm$ 160, 2050–3550 $\pm$ 160 and 3550–4485 $\pm$ 160 yBP (Fig. 11).
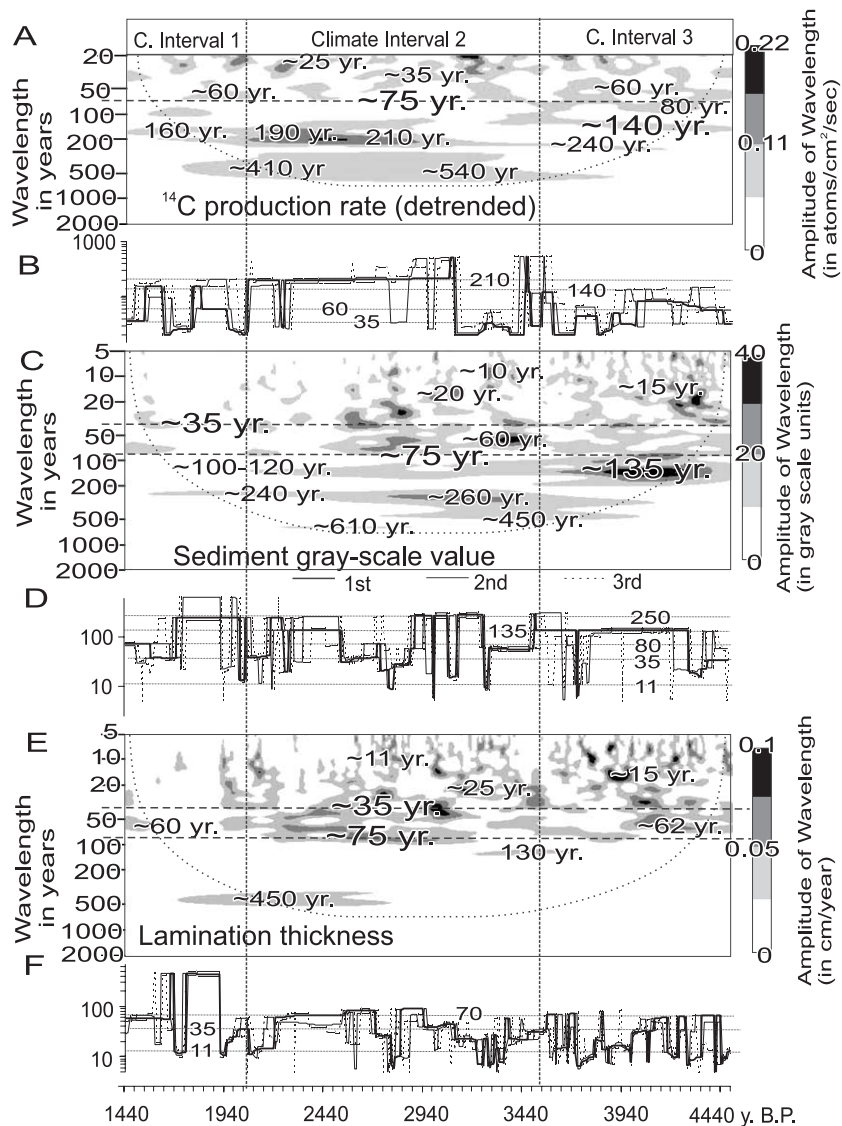
Fig. 10. Wavelet scalograms (A, C, E) with cones of influence, and three major local wavelengths (B, D, F) for sediment gray value and varve thickness of TUL99B-03 (this study), and ^{14}C production rate (after Bond et al., 2001). Note that major changes in the periodicities occur in all three signals at ~3550 yBP (dashed line) and a minor shift occurs at ~2050 yBP (dashed line) that separate climate intervals 1, 2 and 3. Horizontal dashed lines are markers for some important wavelengths. For technical details, see Fig. 5.

The interval from 1440 to 2050 yBP is characterised by a 56-year cyclicity in lamination thickness and a ~76-year cyclicity in sediment color (Fig. 12A). A secondary periodicity in sediment color occurs in the 18–22- and 36-year frequency bands, and similarly, at the 18-, 28-, and 36-year wavelengths in lamination thickness. The strong red noise (high peak at 614-year trend) is very likely a result of the use of linearly

interpolated data in the sedimentary record through the 1760–1920±160 yBP interval where there was a combination of missing core and/or poor image quality.

The interval between 2050 and 3550±160 yBP is characterised by a long-term 300±40-year cyclicity in sediment color and a ~500±120-year cyclicity in lamination thickness. The ~500-year cycle repeats
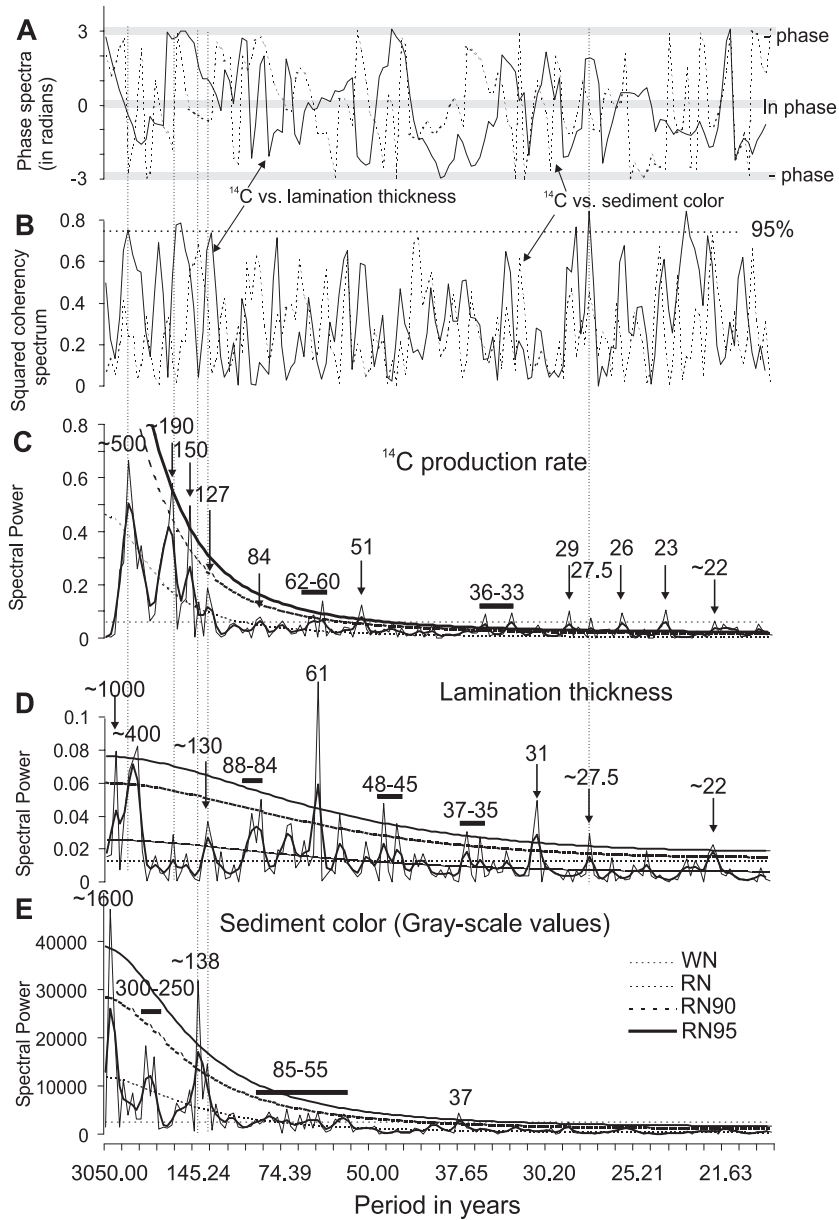
Fig. 11. Spectral (C, D, E) (periodograms—thin line, spectral power from 1/5-lag Hamming-window—bold line) and cross-spectral analysis (A, B) (square coherency and phase spectrum) for (E) sediment gray value and (D) lamination thickness of TUL99B-03 (this study), and (C) ^{14}C production rate (after Bond et al., 2001) for the interval from 1440 to 4600 yBP in 10-year-averaged time intervals. RN—red noise levels calculated from white levels, RN90 and RN95 red noise calculated from re-sampling method, WN—average variance of spectral analysis (=white noise). Black bars indicate ranges of significant period bands. Vertical dashed lines mark wavelength bands with significant cross-correlation (see (B)) to ^{14}C production rate.

itself only three times in this interval and is thus statistically not robust. Nevertheless, its coeval occurrence with a ~400–500-year ^{14}C production

cycle (Fig. 11) indicates a possible non-periodic, but deterministic, relationship between cosmic ray flux/ solar variability and the Effingham Inlet sedimentary

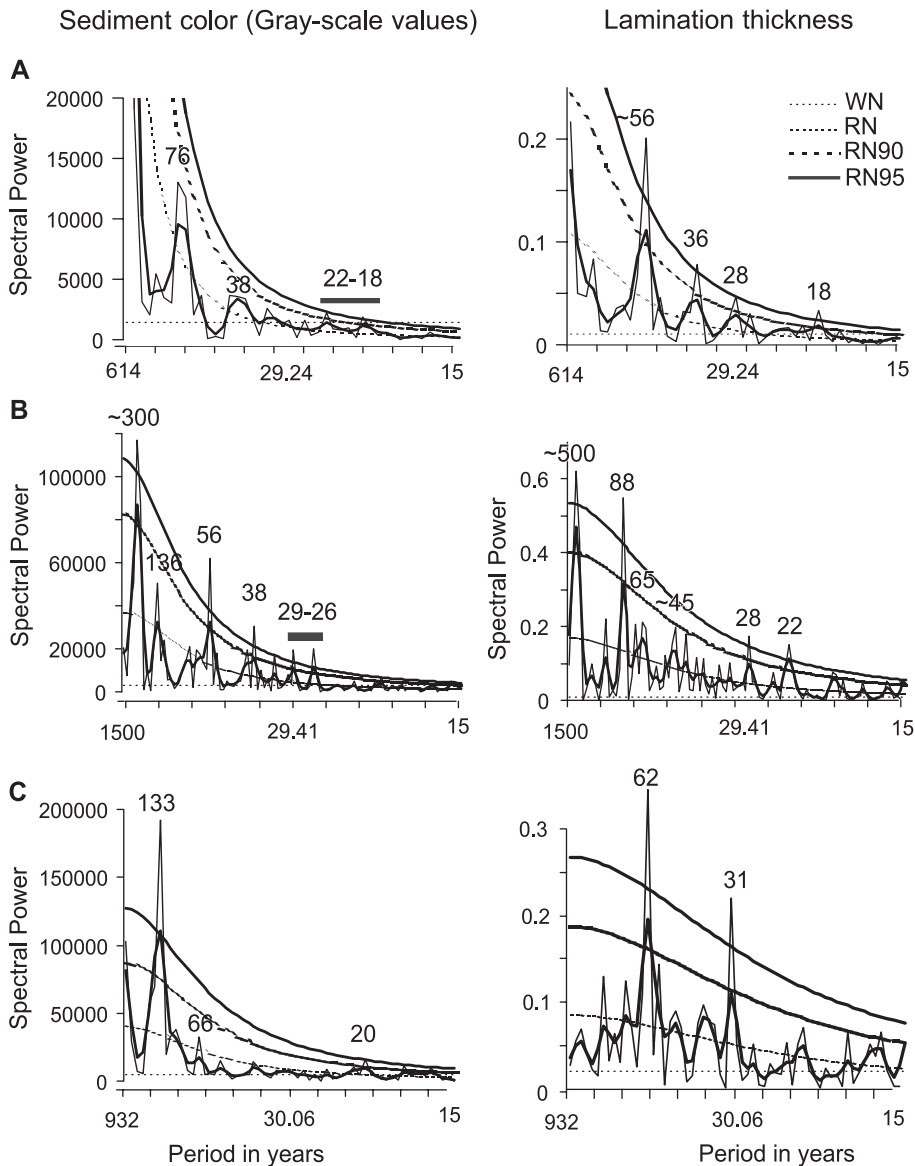Sediment color (Gray-scale values)   Lamination thickness

Fig. 12. Spectral (periodograms—thin line, spectral density from 1/5-lag Hamming-window—bold line) of lamination thickness and sediment color of TUL99B-03, for noise levels, see Fig. 11. Black bars indicate ranges of significant period bands: (A) Interval from 1440 to 2050 yBP. (B) Interval from 2050 to 3550 yBP. (C) Interval from 3550 to 4485 yBP.

record. A secondary 55.5±1.0-year cycle occurs in sediment color and an 88.0±2.5-year frequency band in the lamination thickness. Shorter significant wavelengths (22, 26–29, 38, 45, 65, and 136 years) are non-correlative between both records (Fig. 12B).

The interval between 3550 and 4485 yBP is characterised by a dominant 133±16-year fre-

quency band in sediment color (Fig. 12C). The 62–66-year frequency band is significant in both records (Fig. 12C) and also occurs in the ^{14}C productivity record (Fig. 10A), suggesting that this periodicity is during this time interval well developed in the sedimentation and driven by cosmic ray flux/solar activity variability. The weaker 31- and

15-year cycles may be results of period doubling of the ~62-year periodicity.

5. Interpretation and discussion

Wavelet and spectral time series analysis of lamination thickness and sediment color (gray-scale values) data, derived from X-ray images of Core TUL99B-03 in anoxic Effingham Inlet, revealed a wide spectrum of stationary and non-stationary climate cycles. These annual and longer cycles could be linked to regional NE Pacific and global late Holocene climate changes, as well as to variability in solar irradiance. In addition, the similarity of this NE Pacific record to the ice drift debris record in the North Atlantic (Bond et al., 2001) suggests that at even longer return times of >1000 years, the northern hemisphere temperature regime is positively linked to solar irradiance levels (Hameed and Lee, 2003).

Time-series analysis and graphical correlation revealed three major depositional/climatic intervals (Climate Interval 3–3550–4485±160 yBP; Climate Interval 2–2050–3550±160 yBP; Climate Interval 1–1440–2050±160 yBP), which were discriminated based on distinct changes in sedimentation rate (lamination thickness) and the composition of the sediments (i.e. sediment color) (Table 2). These

intervals correlated well with other geological and paleoclimate records from coastal British Columbia (e.g., Pellat and Mathewes, 1997; Nederbragt and Thurow, 2001).

5.1. Climate Interval 3: 3550–448±160 yBP

A detailed analysis of the diatom floras from this core indicates that prior to ~3600 yBP oceanic conditions were relatively constant and favorable to annual seasonal upwelling (Chang et al., 2003; Hay and Pienitz, submitted for publication). The pollen record of British Columbia indicates that the climate was also relatively warmer and drier during this interval, although estimates of when these conditions terminated vary from ~4000 to ~3200 yBP (Pellat et al., 2001). This transition to cooler and wetter conditions also coincides with the well-documented neoglacial advance of the Tiedemann Glacier at ~3300 yBP (Pellat and Mathewes, 1997). There was also a dramatic increase in hematite stained grains (ice drift indicators) in the NE Atlantic at this time as well suggesting that the cooling was at least hemispheric in extent (Bond et al., 2001).

The time series analyses results presented here suggest that the climatic patterns that ultimately resulted in the cooler and wetter conditions after ~3550±160 yBP were marked by a significant shift

Table 2
Summary of cyclicity (in years) in observational and sedimentary records

Observation period	Synonymon	20-year sunspot	Gleissberg			
0–400 yBP	Solar irradiance	22	73–90			
	Synonymon	BDO	PDO/AL/ Interdecadal	VLF/ Multidecadal	Multidecadal	Centennial
0–400 yBP	Global climate	18–25, 29	15–35	50–90	90–150	200–500
0–150 yBP	Oceanography/ Climate NE Pacific	20–31	30–70	60–80		
1440–2050 yBP	14C production rate	20, 25	35	60	97, 150	200
	Sediment color	18–22	38	56, 70–76		220–270, 610
	Varve thickness	28	36	58–76		400–500
2050–3550 yBP	14C production rate	22, 28	35			190–210, 410, 520
	Sediment color	22, 26–29	38	56	136–160	250–300, 500
	Varve thickness	22, 28	45	65–90	136	210, 500
3550–4500 yBP	[14]C production rate	25	32	60, 72, 80	130–150	
	Sediment color	20–22	35	58, 72, 82	135	
	Varve thickness		31	60–70	133	500

from higher-frequency (~60–140 years) to lower-frequency (~190–500 years) climate cycle patterns (Figs. 10E,F and 12). The synchronous shift in ^{14}C production rates from a ~140- to a ~190-year cyclicity (Fig. 10A,B) at this transition suggests that changes in solar activity may be responsible for the climate deterioration. We hypothesize that weakened higher-frequency solar activity pulses, particularly at the Gleissberg cycle band (~75–90 years) lead to re-organization of the climate system in the NE Pacific resulting in a weakening of lower frequency PDO cycles. This hypothesis is corroborated by the presence of ~60–65-year cycles in the cosmogenic nuclide record (Figs. 10 and 11) that match up well with the lower frequency PDO cycles found in the core.

5.2. Climate Interval 2: 2050–3550±160 yBP

The cooler and wetter conditions that prevailed during this climate interval are well documented in many British Columbia palynological studies (Pellat et al., 2001). In Effingham Inlet, an increase in the number of non-laminated units through this interval in Core TUL99B-03 indicates a departure from the normally anoxic conditions conducive to preserving laminated sediments (Chang et al., 2003). Under certain conditions, it is possible for bottom waters of the inner basin to be briefly aerated by deeply upwelled and oxygenated waters. The lower-frequency (190–600 years) cycles that prevailed in Effingham Inlet through Climate Interval 2 correlates well with global solar irradiance records (Bond et al., 2001) and the ^{14}C periodicity (Fig. 10A,B). Major documented non-periodically occurring lows in solar irradiance at ~2350, ~2750 and ~3350 yBP (Bond et al., 2001) and peaks in ^{14}C production rate (Fig. 9E) are represented in the core by thick and dark mineral-rich clay (Fig. 9F,G) that were laid down during a series of unusually wet winters. This correlation suggests that strong changes in solar irradiance levels triggered unusually high levels of precipitation for a time along the NE Pacific coast. This increase in precipitation in the region can be correlated to intervals of solar minimum when the COA of the AL moved east and the COA of the NPH moved south (Hameed and Lee, 2003) These episodes were probably analogous to the 'Little Ice Age' (LIA) in

Europe. Interpretation of the sedimentary data indicates that during this interval, cold and wet periods occurred with a 400–600-year periodicity.

During the 'cool' Climate Interval 2, a major increase in solar irradiance between ~2450 and 2600 yBP correlates with a period of deposition characterized by unusually thin laminations. It is possible that sedimentation during this interval of maximum solar activity has been influenced by the COA of the AL moving west and the COA of the NPH moving north, similar to the present change in the North Pacific climate (Christoforou and Hameed, 1997; Hameed and Lee, 2003). This indicates that despite the overall cool and wet conditions that prevailed through Climate Interval 2 there was at least this one extended episode of dryer conditions that resulted in decreased sediment supply to Effingham inlet. Since the inverse correlation between lamination thickness and solar irradiance intensity is the most prominent long-term feature in the Climate Interval 2 sedimentary record it must be concluded that both the intensity and the periodicity of solar activity affect the locations of COAs (i.e. AL and NPH) and therefore are dominant controlling factors on sedimentation.

5.3. Climate Interval 1: 1440–2050±160 yBP

Palynological evidence indicates that modern climate conditions, characterized by a slight warming, developed in British Columbia around 2000 yBP (Pellat and Mathewes, 1997). This transition is marked in the cyclostratigraphic record in core TUL99B-03 by a significant weakening of the lower-frequency (~200–500 years) climate cycle pattern that dominated Climate Interval 2. A 56–90-year cycle is prominent in the sedimentary record, as was also the case during Climate Interval 3 (Fig. 12C), providing corroborative evidence of the reoccurrence of a similar climate regime. This 56–90-year cyclicity also re-occurs in the solar irradiance record indicating that this change was a global phenomenon (Fig. 10A). The presence of generally thin laminated sediments through the Climate Interval 1 portion of the core indicates primarily anoxic to dysoxic conditions, with only a few oxic events recorded, and suggests that there was a high degree of vertical stratification with a warmer SST (Fig. 5, Table 2). This sedimentary record and the global nuclide record indicate that extreme cold/wet and warm/dry

periods of durations longer than 20 years did not occur during Climate Interval 1.

5.4. Influence of PDO, AL and solar activity cycles on climate in the NE Pacific

An intense, but non-persistent cyclicity in the ~18–29-year frequency-band (Figs. 11 and 12) is characterized primarily by variation in sediment lamination thickness and in the ^{14}C production rate, that is not evident from other records in the NE Pacific, and is in the range of variability of the ~22-year sunspot cycle. However, the occurrence of this cycle is too sporadic and the uncertainty associated with sedimentation rate fluctuation at high-resolution (<30-year wavelength) is too high in the core studied to infer a particular controlling factor such as solar influence.

The sedimentary record of core TUL99B-03 indicates that during the relative warm intervals (1440–2050, 3550–4485 yBP) interdecadal ~35 (31–38)-year cycles appear (Fig. 12), probably representing different intensity stages of the AL and the high periodicity PDO variant (Mantua et al., 1997; Minobe, 1997, 1999). High-periodicity PDOs are associated with a more intense AL resulting in a weak transport of moisture by westerlies into the NE Pacific region while low-periodicity PDOs result in cooler and wetter conditions. We conclude that diminished AL activity between 2050 and 3550 yBP resulted in lower SST and enhanced upper layer mixing along the west coast of Vancouver Island. Raspopov et al., 2004 suggests that the ~35-year cyclicity can be explained by a nonlinear positive signal amplification of the ~88-year Gleissberg and the ~22-year Schwabe cycle, because the 35-year cycle would represent the combinatory frequency v of $(v_H - v_G)$.

A ~75–90-year cycle through the interval from 1440 to 3550 yBP, corresponding very well to the ~88-year Gleissberg Solar Cycle (Gleissberg, 1958; Garcia and Mouradian, 1998) occurs frequently and for extended periods of time in the Effingham Inlet sedimentary record. This relationship holds through most of the 1440–3550 yBP record even through major climate shifts at 2050 yBP disrupted most other cycles.

Wavelet analysis of the core record indicates that the ~75–90-year Gleissberg solar cycle was non-stationary though, nearly disappearing during the Climate Interval 2 (2050–3550 yBP) 'cold' period in both the sedimentary and cosmogenic nuclide records (Figs. 11 and 12B). The same phenomenon occurred during the Maunder minimum (1640–1710 AD) when solar sunspot activity virtually ceased to exist (Jones et al., 2001; Schindell et al., 2001) only to reappear again during the late 19th and early 20th centuries at the termination of the Little Ice Age (Appenzeller et al., 1998).

In the 'older' warm interval (3550–4485 yBP), the 75–90-year cycle is replaced by a 62–66-year cycle in both the sedimentary and ^{14}C production rate record. It is therefore possible that the Gleissberg solar cycle was not as stationary through the Holocene in contrast to the ~88 year sunspot record pattern observed during the last ~400 years.

The observed relationships between ^{14}C production record and lamination thickness (=sedimentation rate) may be the result of SST changes brought on by solar irradiance fluctuations at the Gleissberg cycle band that led to cycles of wetter/dryer winters and higher/lower spring–summer diatom productivity.

The most intense observed cyclicity in the core was a ~135-year multidecadal cyclicity in cosmogenic [10]Be and sediment records that was prevalent during Climate Interval 3 (Figs. 10–12). Solar cycles drive climate cycles, which controlled precipitation, leading to coeval sedimentary cycles. However, the ~135-year cycle appeared only sporadically and was poorly pronounced through the subsequent climate intervals.

Throughout Climate Interval 2, there was an intense, but non-persistent 190–500-year cyclicity in ^{14}C-production rate and sedimentation, particularly lamination thickness. This cycle band is also found throughout the Northern Hemisphere climatic record (Bond et al., 2001). We therefore conclude that non-periodic variations in solar activity with durations of ~190–500-years significantly affected climatic and oceanographic conditions. Lower levels of solar irradiance associated with cycles at the ~190–500-year wavelength are correlated with increased terrigenous mineral supply. Increased terrigenous mineral supply is in turn correlated to wetter conditions, which resulted in increased runoff. The increased runoff can be linked to increased precipitation, which can be linked to an intensified AL.

A possible explanation for how celestial forcing might impact climate in the NE Pacific is provided by the observed correlation between the 11-year solar cycle and the locations of large-scale atmospheric pressure gyres over the North Pacific Ocean (Christo-forou and Hameed, 1997; Hameed and Lee, 2003). During sunspot maxima, the Center of Action (COA) of the Aleutian Low (AL) pressure system moves west by as much as 700 km, while the COA of the North Pacific High (NPH) pressure system moves north by as much as 300 km. During a sunspot minima, the COA for these pressure systems moves in the reverse direction. Moving of the COA of these important pressure systems has a significant impact on coastal upwelling and climate, which may be significantly amplified through longer return time solar cycles (Carslaw et al., 2002).

The ~190–500-year cycles are also well correlated to major glacier advances in the northern hemisphere, suggesting that solar variability is a major control on centennial-scale climate changes as well (Bond et al., 2001).

6. Conclusions

Solar activity appears to have a major influence on regional and global climate as is recorded in the sedimentation patterns and diatom abundance data from Effingham Inlet, British Columbia. The paleo-climatic data coming out of the present study include evidence of:

(1) A strong cooling in the NE Pacific at ~3550±160 yBP that can be related to a weakening of higher-frequency 50–150-year cycles and the appearance of ~200–500-year cycles.

(2) A ~75–90-year cycle, corresponding very well with the Gleissberg Solar Cycle occurring in much of the Effingham Inlet sedimentary record, even through major climate shifts at 2050 yBP that disrupted most other cycles. The Gleissberg cycle may have been shorter during the 3550–4485 yBP 'warm period', corresponding to a ~60–66-year cycle observed in both the sedimentary and ^{14}C production rate records.

(3) Additional cycles (e.g., 31–38, and 18–28 years) forming a significant portion of ^{14}C production

(i.e. solar activity) variability that can be correlated with modern climate phenomenon in the NE Pacific such as the AL and PDO. These cycles correlate particularly well with the variability in annual lamination thickness and sediment color during Climate Interval 3 (3550–4485 yBP).

(4) At least three events that can be correlated to lower solar activity; at ~2350, 2750 and ~3350 yBP. These climatic intervals were characterized by unusually wet conditions that resulted in deposition of intervals of unusually thick, clay-rich annual laminations. These events may be related to an intensification of the AL related to the eastward migration of the COA of the AL during intervals of solar minima.

(5) An unusually long episode (~150 years) of high solar activity between ~2450 and 2600 yBP that can be related to dry conditions in the NE Pacific that resulted in deposition of an interval of thin annual laminations. Deposition during this climatic event may have been the result of the influence of an interval of solar maxima when the COA of the AL would have moved west and the COA of the NPH moving north.

Acknowledgements

References

Appenzeller, C., Stocker, T.F., Anklin, M., 1998. North Atlantic oscillation dynamics recorded in Greenland ice cores. Science 282, 446–449.

Blais-Stevens, A., Bornhold, B.D., Kemp, A.E.S., Dean, J.M., Vaan, A.A., 2001. Overview of Late Quaternary stratigraphy in Saanich Inlet, British Columbia: results of Ocean Drilling Program Leg 169S. Mar. Geol. 174, 3–20.

Bond, G., Kromer, B., Beer, J., Muscheler, R., Evans, M.N., Showers, W., Hoffmann, S., Lotti-Bond, R., Hajdas, I., Bonani, G., 2001. Persistent solar influence on North Atlantic climate during the Holocene. Science 294, 2130–2136.

Carslaw, K.S., Harrison, R.G., Kirkby, J., 2002. Cosmic rays, clouds and climate. Science 298, 1732–1737.

Chang, A.S., Patterson, R.T., McNeely, R., 2003. Seasonal sediment and diatom record from late Holocene laminated sediments, Effingham Inlet, British Columbia, Canada. Palaios 18, 477–494.

Christoforou, P., Hameed, S., 1997. Solar cycle and the Pacific 'centers of action'. Geophys. Res. Lett. 24, 293–296.

Dallimore, A., 2001. Late Holocene geologic, oceanographic and climate history of an anoxic fjord: Effingham Inlet, West Coast, Vancouver Island, PhD Dissertation, Carleton University, Ottawa, Ontario.

Dean, W.E., 2000. The Sun and Climate, USGS Fact Sheet FS-095-00, 6 pp.

Favorite, F., Dodimead, A.J., Nasu, K., 1976. Oceanography of the subarctic Pacific region, 1960–71. Bull.-Int. N. Pac. Fish. Comm. 33 (187 pp.).

Francis, R.C., Hare, S.R., Hollowed, A.B., Wooster, W.S., 1998. Effects of interdecadal climate variability on the oceanic ecosystems of the NE Pacific. Fisheries Oceanogr. 7, 1–21.

Friis-Christensen, E., Lassen, K., 1991. Length of the solar cycle: an indicator of solar activity closely associated with climate. Science 254, 698–700.

Garcia, A., Mouradian, Z., 1998. The Gleissberg Cycle of minima. Sol. Phys. 180, 495–498.

Gedalof, Z., Smith, D.J., 2001. Interdecadal climate variability and regime-scale shifts in Pacific North America. Geophys. Res. Lett. 28, 1515–1518.

Gleissberg, W., 1958. The eighty-year sunspot cycle. J. Br. Astron. Assoc. 68, 1148–1152.

Haigh, J.D., 1994. The role of stratospheric ozone in modulating the solar radiative forcing of climate. Nature 370, 544–546.

Hameed, S., Lee, J.N., 2003. Displacements of the Aleutian Low and the Hawaiian High pressure systems during the solar cycle. Eos Transactions, American Geophysical Union 84, Fall Meeting Supplemental, Abstract SH11E-03.

Hay, M.B., Pienitz, R., submitted for publication. Diatom record of late Holocene oceanography and climate along the west coast of Vancouver Island, British Columbia (Canada). Quaternary Research.

Jones, P.D., Osborn, T.J., Briffa, K.R., 2001. The evolution of climate over the last millennium. Science 292, 662–666.

Mann, M.E., Park, J., Bradley, R.S., 1995. Global interdecadal and century-scale climate oscillations during the past five centuries. Nature 378, 266–270.

Mantua, N.J., Hare, S.R., Zhang, Y., Wallace, J.M., Francis, R.C., 1997. A Pacific interdecadal climate oscillation with impacts on salmon production. Bull. Am. Meteorol. Soc. 78, 1069–1079.

Minobe, S., 1997. A 50–70 year climatic oscillation over the North Pacific and North America. Geophys. Res. Lett. 24, 683–686.

Minobe, S., 1999. Resonance in bidecadal and pentadecadal climate oscillations over the North Pacific: role in climatic regime shifts. Geophys. Res. Lett. 26, 855–858.

Nederbragt, A.J., Thurow, J., 2001. A 6,000 year varve record of Holocene sediments in Saanich Inlet, British Columbia, from digital sediment colour analysis of ODP Leg 169S cores. Mar. Geol. 174, 95–110.

Pellat, M.G., Mathewes, R.W., 1997. Holocene tree line and climate change on the Queen Charlotte Islands, Canada. Quat. Res. 48, 88–99.

Pellat, M.G., Hebda, R.J., Mathewes, R.W., 2001. High-resolution Holocene vegetation history and climate from Hole 1034B, ODP leg 169S, Saanich Inlet, Canada. Mar. Geol. 174, 211–222.

Raspopov, O.M., Dergachev, V.A., Kolstroem, T., 2004. Periodicity of climate conditions and solar variability derived from dendrochronological and other palaeoclimatic data in high latitudes. Palaeogeography, Palaeoclimatology, Palaeoecology. vol. 209, pp. 127–139.

Schaaf, M., Thurow, J., 1994. A fast and easy method to derive highest-resolution time-series datasets from drillcores and rock samples. Sediment. Geol. 94, 1–10.

Schindell, D.T., Schmidt, G.A., Mann, M.E., Rind, D., Waple, A., 2001. Solar forcing of regional climate change during the Maunder Minimum. Science 294, 2149–2152.

Soon, W.H., Posamentier, E.S., Baliunas, S.L., 1996. Inference of solar irradiance variability from terrestrial temperature changes, 1880–1993: an astrophysical application of the Sun–climate connection. Astrophys. J. 472, 891–902.

Stuiver, M., Reimer, P.J., 1993. Extended ^{14}C database and revised CALIB radiocarbon calibration program. Radiocarbon 35, 215–230.

Stuiver, M., Reimer, P.J., Bard, E., Beck, J.W., Burr, G.S., Hughen, K.A., Kromer, B., McCormac, F.G., Plicht, J., Spurk, M., 1998a. INTCAL 98 Radiocarbon age calibration 24,000–0 cal BP. Radiocarbon 40, 1041–1083.

Stuiver, M., Reimer, P.J., Braziunas, T.F., 1998b. High-precision radiocarbon age calibration for terrestrial and marine samples. Radiocarbon 40, 1127–1151.

Svensmark, H., 1998. Influence of cosmic rays on Earth's climate. Phys. Rev. Lett. 81, 5027–5030.

Thomson, R.E., 1981. Oceanography of the British Columbia coast. Can. Spec. Publ. Fish. Aquat. Sci. 56 (291 pp.).

Torrence, C., Compo, G.P., 1998. A practical guide to wavelet analysis. Bull. Am. Meteorol. Soc. 79, 61–78.

Ware, D.M., 1995. A century and a half of change in the climate of the NE Pacific. Fisheries Oceanogr. 4:4, 267–277.

Ware, D.M., Thomson, R.E., 2000. Interannual to multidecadal timescale climate variations in the Northeast Pacific. J. Climate 13, 3209–3220.